PHYSICAL REVIEW B VOLUME 32, NUMBER 8 15 OCTOBER 1985

Indexing problems in quasicrystal diffraction

Veit Elser
AT&T Bell Laboratories, Murray Hill, New Jersey 07974
(Received 26 April 1985)

Various features of quasicrystal diffraction patterns are discussed. The projection scheme is used throughout and applied in some detail to the pattern formed by icosahedral Al-Mn. Comparison with the diffraction pattern formed by the vertices of a three-dimensional Penrose tiling leads to the value 4.60 Å for the rhombohedron edge length.

The icosahedral phase of $Al_{0.86}Mn_{0.14}$ recently discovered by Shechtman *et al.*[1] provides a rare challenge to crystallographers. While it is almost certain that some application of their art is necessary to unravel the detailed atomic positions, such an endeavor requires a major revision of the classical formulation of the problem. The incomplete state of present knowledge can be appreciated when we consider the fact that even for the most complicated cases of ordinary crystal structure (i.e., large unit cells) at least the determination of the lattice parameters is an absolutely straightforward task. The Al-Mn icosahedral phase defies even this first step of the structure determination. There is no indication that in either real or reciprocal space its structure can be described by simply specifying the dimensions and angles of some periodically repeating unit. Thus it appears necessary that one incorporate into crystallography the possibility of ordered *aperiodic* structures.[2–7]

The objective of this paper is to discuss characteristic features of the diffraction pattern formed by structures projected from higher-dimensional periodic lattices (quasicrystals). Some formalism for the special case of the icosahedral quasicrystal is developed, and we even go so far as to compute the "quasilattice constant" for icosahedral Al-Mn. No attempt has been made to give precise mathematical definitions; for these the reader is referred to a separate publication.[5]

I. QUALITATIVE PROPERTIES OF QUASICRYSTAL DIFFRACTION

Independent of the issue of symmetry, there are some qualitative differences between quasicrystal diffraction (QCD) and ordinary crystal diffraction (OCD). The pattern formed by OCD is an infinite lattice of Bragg peaks of roughly equal intensity. In fact, if we put a single pointlike atom inside each primitive Bravais cell, then the intensities will be exactly equal. Smearing out the charge density of the atom or, more generally, modifying the charge density by adding more atoms to the primitive cell, only modulates intensities without moving or adding peaks. The most prominent of these effects is due to atomic form factors which cause intensities to decay rapidly beyond some radius in reciprocal space.

The pattern of Bragg peaks formed by QCD is a dense filling of reciprocal space.[3–7] The nature of each peak is in all respects identical to the δ-function peak of OCD. By this we mean that the intensity of a peak is proportional to the volume and has zero width in the absence of strain. Moreover, all the mechanisms that can broaden an OCD peak will apply also to a QCD peak. Nevertheless, one now has the remarkable property that within any volume of reciprocal space there are infinitely many peaks. Fortunately, most of these peaks are extremely weak, making it possible to distinguish individual ones. In principle it is possible to surround a given peak by a sequence of smaller and smaller volumes such that the intensities of all the other peaks in the volume become arbitrarily weak. This suggests there is an interesting new kind of decay in peak intensity unrelated to anything in OCD. Of course it is still possible to modulate intensities in the conventional way by modifying the charge density in the "quasicrystal unit cell." For example, the atomic form factor effects will still continue to play a role and will vary *continuously* with g, the position in reciprocal space. We thus distinguish "g-dependent" effects from the more subtle effects that occur in arbitrarily small volumes of reciprocal space wherein g is virtually constant. For the latter we use the expression "$g_\perp$ dependent."

II. PROJECTIONS FROM HIGHER DIMENSIONS

A natural way of representing the quasicrystal diffraction pattern is by means of projecting an ordinary higher-dimensional reciprocal lattice.[4–8] To emphasize the projected nature of the physical momentum we will adopt the notation $g_\parallel$ in place of g, and reserve the use of g for the higher-dimensional lattice. Figure 1 shows the projection $g=(g_\parallel,g_\perp)$ of a two-dimensional lattice into a one-dimensional subspace. Provided that the space of "physical" reciprocal vectors given by the $g_\parallel$ axis is incommensurate with the lattice, the projections will be dense. We notice that two projections with very nearly equal values of $g_\parallel$ can arise only at the expense of having their corresponding lattice vectors widely separated in the orthogonal $g_\perp$ direction. The qualitative features of the quasicrystal diffraction pattern can thus be understood if one assumes that the intensities decay with the magnitude of $g_\perp$.

If experimental resolution is represented by the pair of dashed lines in Fig. 1, then only the lattice vectors be-

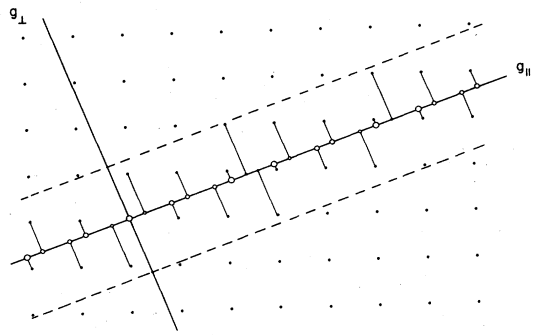

FIG. 1. Projection of a two-dimensional reciprocal lattice into one dimension. Intensities are represented by the sizes of the circles and decay with the magnitude of $g_\perp$. Dashed lines represent experimental resolution.

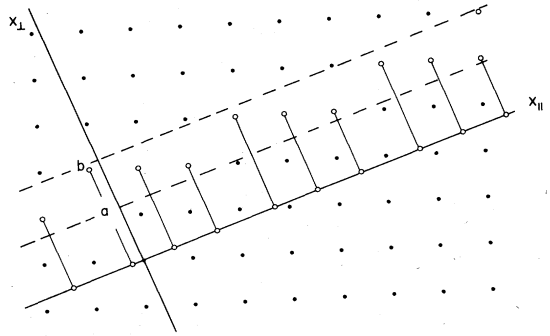

FIG. 2. A one-dimensional quasicrystal generated by projecting a two-dimensional periodic lattice. Only the points between the dashed lines are projected onto the $x_\parallel$ axis.

tween these lines give rise to observable peaks. Increasing the resolution of the spectrometer has the effect of moving the dashed lines outward to a larger $|g_\perp|$, thus filling in the regions between peaks on the $g_\parallel$ axis with even weaker peaks.

The detailed mode of decay of intensities with increasing $|g_\perp|$, what we have called $g_\perp$-dependent behavior, is determined by the structure of the quasicrystal. A particularly simple quasicrystal structure is again obtained by projecting a higher-dimensional lattice.[2,4–8] We may continue the example above by considering the two-dimensional lattice of vectors x reciprocal (in the conventional sense) to the lattice of Bragg vectors g. This gives us a two-dimensional crystal lattice of the usual kind. A simple one-dimensional quasicrystal results if we now project these lattice points into a one-dimensional incommensurate space represented by the $x_\parallel$ axis in Fig 2. Because we want the projected points to define a structure of atoms of nonvanishing size, we avoid a dense pattern by restricting ourselves to only those lattice points which lie between two other lines (shown as dashed in Fig. 2) parallel to the $x_\parallel$ axis. The positions of these lines can be specified in terms of their intersection with the orthogonal axis at $x_\perp=a$ and $x_\perp=b$. A finite quasicrystal having N projected points is of course bounded in the $x_\parallel$ direction as well.

By choosing the same orientation for the $x_\parallel$ and $g_\parallel$ axes in their respective lattices, the following identity holds for any pair of vectors $x=(x_\parallel,x_\perp)$ and $g=(g_\parallel,g_\perp)$:

$$1=e^{ix\cdot g}=e^{ix_\parallel g_\parallel}e^{ix_\perp g_\perp}\ . \tag{1}$$

If for simplicity one places identical pointlike atoms at each of the projections $x_\parallel^n$, $n=1,2,\ldots,N$, then the (one-dimensional) structure factor $S(g_\parallel)$ is given by the sum

$$S(g_\parallel)=\sum_{n=1}^{N}e^{ix_\parallel^n g_\parallel}=\sum_{n=1}^{N}e^{-ix_\perp^n g_\perp}\ . \tag{2}$$

The second step was accomplished using identity (1) and demonstrates that it is useful to know the distribution $\rho(x_\perp)$ of the values $x_\perp^n$. From Fig. 2 it is clear that these must fall inside the interval (a,b). In fact, the incommensurate nature of the projection has the effect that the actual distribution in the limit $N\to\infty$ is dense and uniform on the interval (a,b). According to (2), the Fourier transform of $\rho(x_\perp)$ gives the structure factor

$$S(g_\parallel)=N\frac{\sin z}{z},\quad z=\tfrac{1}{2}|a-b|g_\perp\ . \tag{3}$$

In the idealized situation under consideration we see that the intensities are only $g_\perp$ dependent. If all the atomic charges were spread out in the same way, the net effect on (3) would simply be to multiply it by a function of $g_\parallel$. More complicated decorations of the quasicrystal are also possible and lead to structure factors having a more complex $g_\parallel$ and $g_\perp$ dependence.

The rather slow $g_\perp$-dependent decay of intensities given by (3) is due to the sharp discontinuities of the distribution $\rho(x_\perp)$ at $x_\perp=a$ and $x_\perp=b$. The shape of the distribution will be different if the method for selecting the x-lattice points is changed. For example, one might consider the possibility of allowing the dashed lines in Fig. 2 to wander or have small oscillations with some distribution of amplitude in the $x_\perp$ direction (see Fig. 3). Consequently, it is not inconceivable to have a Gaussian $\rho(x_\perp)$, in which case the $g_\perp$-dependent decay of intensities would be much faster (i.e., also Gaussian).

To see what effect these changes have on the actual quasicrystal we first reconsider the original construction with $|a-b|$ chosen so that the dashed lines span exactly one cell of the lattice, corner to corner (see Fig. 4). This

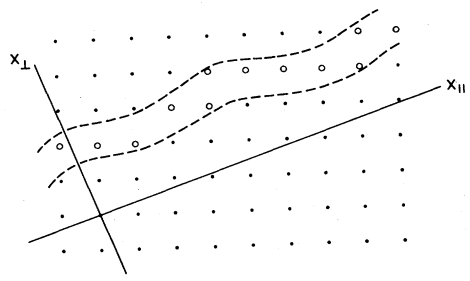

FIG. 3. One possible way to generalize the selection of lattice points.

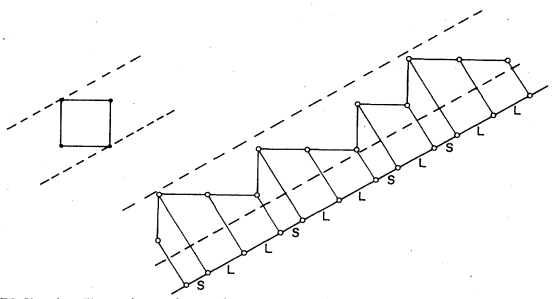

FIG. 4. By choosing the separation between the dashed lines as shown on the left, the selected lattice points form a staircase which projects into a sequence of long and short intervals.

creates the nice property that there now exists a unique lattice path ("staircase") that is bounded by the two lines and, in some sense, best approximates the incommensurate slope. Notice that the points of the quasicrystal form a sequence of long and short line segments.

We can now ignore the dashed lines of the construction and consider modifications of the staircase itself. By projecting respectively into the $x_{\parallel}$ and $x_{\perp}$ axes, it is possible to follow the resulting changes in both the quasicrystal and the distribution $\rho(x_{\perp})$. The basic transformation modifies a step in the staircase (see Fig. 5) and amounts to swapping long-short combinations in the quasicrystal. Suitable sequences of these transformations are capable of generating the whole family of staircases having a fixed average slope. Borrowing the terminology of interface physics one might describe the original staircase as a "facet" which is "roughened" by a step transformation.[9]

Completely analogous constructions apply to d-dimensional quasicrystals projected from D dimensions, including the icosahedral quasicrystal with $d=3$ and $D=6$.[2,4–6] Describing the higher-dimensional case in detail gets rather involved geometrically and we only mention the close analogy with the staircase picture above. It is possible to distinguish between quasicrystals that are optimal approximations of d-dimensional hyperplanes and rough versions thereof.[9] When projected into the orthogonal $D-d$ dimensions analogous to the $x_{\perp}$ axis, these will lead to different distributions ρ. As before, the Fourier transform of ρ is directly related to the $g_{\perp}$-dependent behavior of peak intensities.

III. ICOSAHEDRAL QUASICRYSTAL DIFFRACTION

Some notation will be useful in sorting out the remarkable icosahedral quasicrystal diffraction pattern exhibited by the recently discovered alloy of rapidly cooled Al and Mn.[1] Just as the Bragg lattice of ordinary crystals is generated by a basis of three vectors, the icosahedral pattern is also generated by a basis $e^i_{\parallel}$, although six in number $(i=1,\ldots,6)$.[10] By this we mean that all the diffraction peaks can be "indexed" or expressed as *integer* linear combinations of these six vectors. Again, it is useful to think of a six-dimensional lattice which has been projected into three dimensions. According to this view, each of the vectors $e^i_{\parallel}$ which generates the diffraction pattern is the projection of a basis vector e^i of the six-dimensional reciprocal lattice:

$$e^i=(e^i_{\parallel},e^i_{\perp}),\quad i=1,\ldots,6\ .$$

This also points out the existence of another set of vectors $e^i_{\perp}$ which span an orthogonal three-dimensional space.

When the vectors $e^i_{\parallel}$ line up with the six fivefold symmetry axes of the icosahedron, the pattern of integer linear combinations also has this symmetry. Although the choice of positive directions is arbitrary, we will stick to the convention shown in Fig. 6 with $e^1_{\parallel}$ a polar vector surrounded in cyclic order by $e^2_{\parallel},e^3_{\parallel},\ldots,e^6_{\parallel}$. Within their own "pseudospace," the orthogonal set of vectors $e^i_{\perp}$ also form an icosahedral set. However, having already made a definite choice for the vectors $e^i_{\parallel}$, we must choose the vectors $e^i_{\perp}$ as shown in Fig. 6.[5] We notice that (1) the directions of $e^2_{\perp},e^3_{\perp},\ldots,e^6_{\perp}$ relative $e^1_{\perp}$ are reversed and (2) the cyclic ordering of $e^2_{\perp},e^3_{\perp},\ldots,e^6_{\perp}$ is changed. If we take all the vectors $e^i_{\parallel}$ and $e^i_{\perp}$ to be unit vectors,[11] then all the essential geometry can be summarized by the scalar products

$$e^i_{\parallel}\cdot e^j_{\parallel}=-e^i_{\perp}\cdot e^j_{\perp}=\pm\frac{1}{\sqrt{5}}\quad(i\neq j)$$

where the sign is obvious from inspection.

A general Bragg vector may be written as

$$g_{\parallel}=\frac{\pi}{a}\sum_{i=1}^{6}n_i e^i_{\parallel}\ , \tag{4}$$

where the n_i are integers and may be thought of as indices. Here the scale is provided by the inverse of a, the "quasilattice constant." More precisely, a represents the edge length of the rhombohedral cells that make up the three-dimensional Penrose tiling.[5] For each Bragg vector given by (4), there corresponds a unique partner in pseudospace:

$$g_{\perp}=\frac{\pi}{a}\sum_{i=1}^{6}n_i e^i_{\perp}\ .$$

FIG. 5. An elementary step transformation interchanges adjacent long and short intervals.

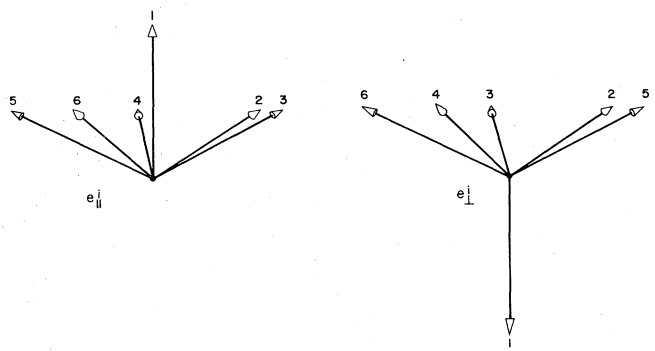

FIG. 6. The icosahedral basis vectors in physical space and pseudospace.

In the primitive quasicrystal, with identical pointlike atoms at the vertices of the rhombohedral cells, the intensities are strictly functions of $g_\perp$. Decorating the cells with a more general charge distribution will add some kind of $g_{||}$ dependence to the intensities as well.

The significance of the "pseudo-Bragg-vector" $g_\perp$ can be understood in the following way. It is quite easy to show that suitable (integral) combinations of the basis set $e^i_{||}$ will produce Bragg vectors densely in a region of $g_{||}$ space. If this region is small, then the intensity variations due to $g_{||}$-dependent effects will likewise be small. If one now examines the pseudospace partners of this local group of Bragg vectors, one finds they are spread out over a large region in $g_\perp$ space. In fact, a converging sequence of vectors in $g_{||}$ space will actually diverge in $g_\perp$ space. Thus the dense set of Bragg peaks in a small region will have widely different intensities due to large variations in $g_\perp$.

Intensity values for the most prominent Bragg peaks of the primitive icosahedral quasicrystal have been provided in Table I along with the values of $|g_{||}|$ and $|g_\perp|$ (units are such that $a=1$). As in the one-dimensional case, the structure factor is given by the $g_\perp$ Fourier transform of a density ρ which is constant inside a region T and falls abruptly to zero outside of T. The region T turns out to be a triacontahedron,[5,6] a very nearly spherical polyhedron of 30 sides related to the icosahedron. The intensities therefore depend strongly on the magnitude of $g_\perp$ with relatively minute angular variations.

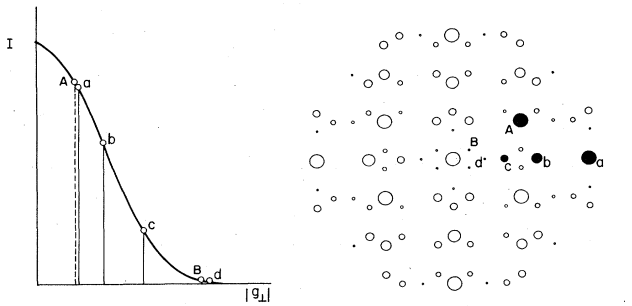

FIG. 7. Progression of $g_\perp$-dependent intensities for an even-parity sequence a,b,c,d and an odd-parity sequence A,B. On the right are shown the corresponding peaks in the diffraction pattern ($g_{||}$ space).

IV. INDEXING THE ICOSAHEDRAL DIFFRACTION PATTERN

Since the diffraction pattern of an ordinary crystal is really just a Bravais lattice, the indexing of such a pattern simply involves obtaining a set of three primitive basis vectors that generate the lattice. A physical scale is easily deduced from the minimum separation of Bragg peaks in the three directions. Understandably, the situation is not nearly this simple for quasicrystals. In that the pattern of peaks is dense, it is not even clear what sets the scale.

A useful way of dealing with the quasicrystal diffraction pattern is through the self-similarity transformations

TABLE I. A listing of peaks for the icosahedral quasicrystal having $|n_{||}|<25$ and $|n_\perp|<3.4$. The intensities given correspond to the primitive quasicrystal with identical point charges at the rhombohedral vertices. The values of $|g_{||}|$ for $Al_{0.86}Mn_{0.14}$ may be obtained by dividing the entries in the first column by $a=4.60$ Å. Labels on the right refer to Figs. 9–11.

$\|n_{||}\|$	$\|n_\perp\|$	$i(n_\perp)$	Parity	n_1	n_2	n_3	n_4	n_5	n_6	Label
0.000	0.000	1.000 000	0	0	0	0	0	0	0	23
3.142	3.142	0.000 043	1	1	0	0	0	0	0	22
5.345	3.303	0.000 800	0	1	1	0	0	0	0	21
7.489	1.768	0.238 225	1	1	1	1	0	0	0	20
8.648	2.042	0.134 874	0	1	1	1	1	0	0	19
11.440	2.701	0.013 211	1	2	1	1	1	0	0	18
12.230	2.887	0.003 335	0	2	1	1	1	1	0	17
13.308	0.742	0.794 142	1	2	1	1	1	1	1	16
13.993	1.262	0.501 572	0	2	2	1	0	0	1	15
14.341	3.385	0.001 817	1	2	2	1	1	0	1	14
15.871	2.172	0.096 895	1	2	2	2	1	0	0	13
16.450	2.400	0.047 775	0	3	1	1	1	1	1	12
18.074	2.981	0.001 404	1	3	2	1	1	1	1	11
18.584	3.151	0.000 001	0	3	2	2	1	0	0	10
19.311	1.464	0.387 990	1	3	2	2	1	0	1	9
19.789	1.784	0.230 827	0	3	2	2	1	1	1	8
21.159	2.512	0.031 390	1	3	3	2	0	0	1	7
21.596	2.711	0.012 579	0	3	3	2	1	0	1	5
22.641	0.780	0.774 703	0	3	3	2	0	0	2	6
22.858	3.237	0.000 253	1	4	2	2	1	1	1	2
23.263	3.394	0.001 633	0	3	3	3	1	0	0	4
23.847	1.932	0.172 020	1	3	3	3	1	0	1	3
24.236	2.185	0.093 199	0	4	2	2	2	1	1	1

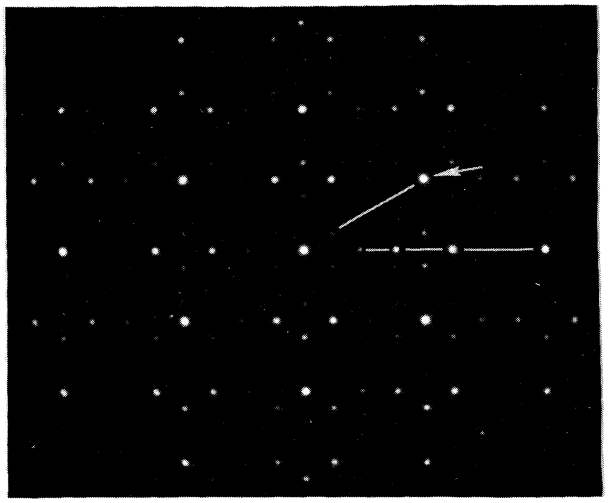

FIG. 8. Even- and odd-parity sequences in the experimental two-fold pattern (Ref. 14). The arrow indicates the peak at 2.896 Å^{-1}.

called inflation and deflation.[12] These transformations define sequences of peaks in $g_{||}$ space with $g_{\perp}$-dependent intensities characteristic of some scale. The rule for inflation is given by the 6×6 matrix

$$M_{ij}=\tfrac{1}{2}\begin{vmatrix} 1 & 1 & 1 & 1 & 1 & 1 \\ 1 & 1 & 1 & -1 & -1 & 1 \\ 1 & 1 & 1 & 1 & -1 & -1 \\ 1 & -1 & 1 & 1 & 1 & -1 \\ 1 & -1 & -1 & 1 & 1 & 1 \\ 1 & 1 & -1 & -1 & 1 & 1 \end{vmatrix}_{ij},$$

which plays a fundamental role in the projection formalism of the icosahedral quasicrystal.[13] Note that M satisfies the polynomial $M^2=M+1$ so that the eigenvalues are $\tau=\frac{1}{2}(1+\sqrt{5})$ and $-\tau^{-1}$. The matrix corresponding to deflation is $M^{-1}=M-1$ which also consists of $\pm\frac{1}{2}$ elements. Here our interest in the matrix M is to define certain half-integral combinations of the icosahedral basis vectors:

$$\begin{aligned}(e_{||}^i)'&=\sum_{j=1}^{6}M_{ij}e_{||}^j=\tau e_{||}^i\ ,\\ (e_{\perp}^i)'&=\sum_{j=1}^{6}M_{ij}e_{\perp}^j=-\tau^{-1}e_{\perp}^i\ .\end{aligned}\tag{5}$$

We see that the vectors $e_{||}^i$ are "inflated" by an amount τ while their pseudospace counterparts are "deflated" by the factor τ^{-1} and reversed.

The matrix M can be used to generate special sequences of Bragg vectors. A convenient shorthand for the Bragg vector (4) is the list of integer indices $(n_1,n_2,\ldots,n_6)$. The matrix M relates a pair of peaks with indices

$$(n_1,n_2,\ldots,n_6)\xrightarrow{M}(n_1',n_2',\ldots,n_6')\ ,$$

where

$$n_i'=\sum_{j=1}^{6}M_{ij}n_j$$

provided of course that the new indices are integers as well. A necessary and sufficient condition for this to be true is that the sum $n_1+\cdots+n_6$ has even parity. The value of this parity along with the list of indices is included with the selection of peaks in Table I. If the parity of a peak is odd, then the appropriate transformation to use in place of M is M^3. This is because $M^3=2M+1$ has only integer elements.

Due to property (5), the effect of these transformations

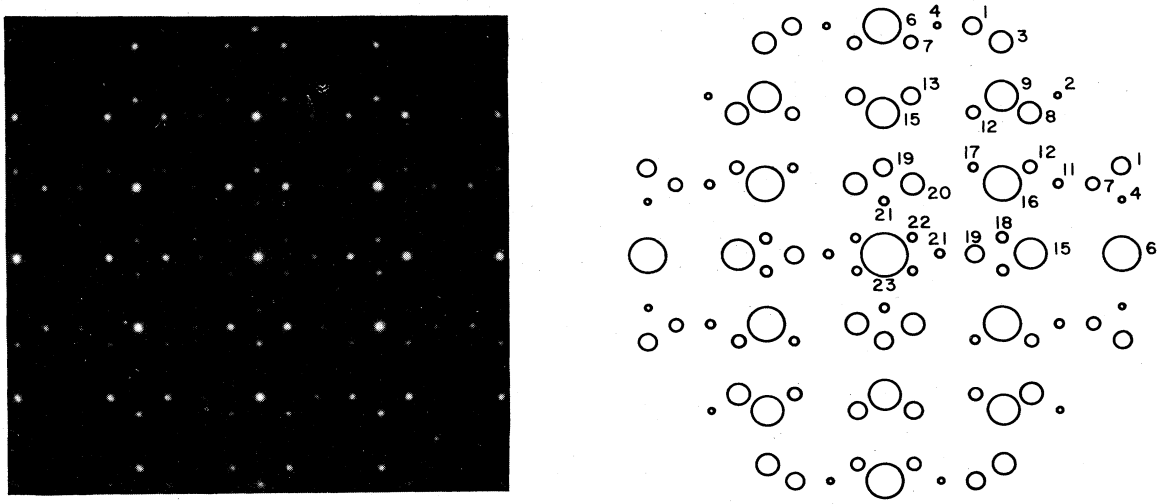

FIG. 9. Comparison of experimental (Ref. 14) and theoretical twofold patterns. The theoretical pattern is that of the primitive icosahedral quasicrystal with a rhombohedral edge length of 4.60 Å. Intensities are represented by the areas of the circles and the numerals refer to the listing of peaks in Table I.

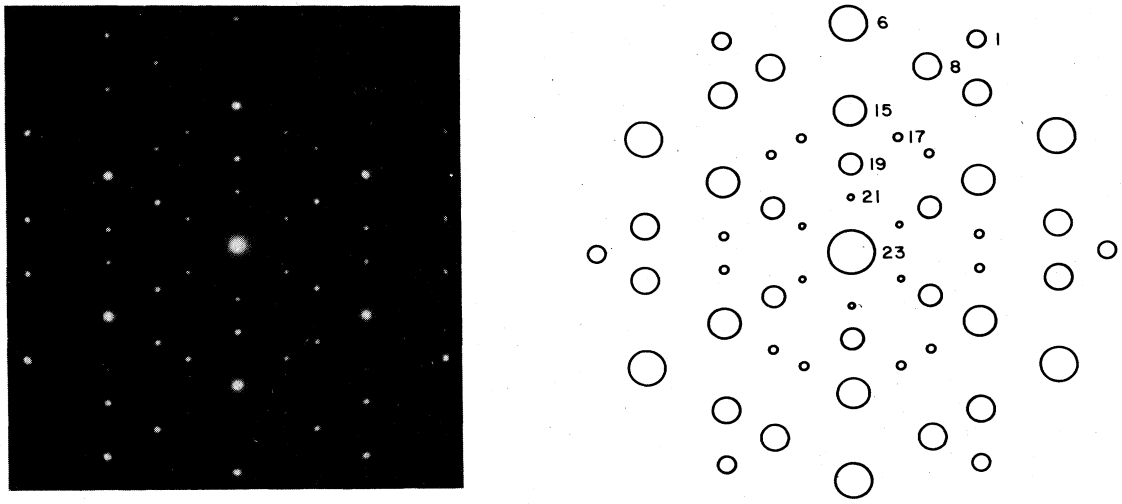

FIG. 10. Same as Fig. 9, but for the threefold pattern.

on the Bragg vectors is very simple. Assuming even parity,

$$g'_{||}=\frac{\pi}{a}\sum_{i=1}^{6} n'_i e^i_{||}$$

$$=\frac{\pi}{a}\sum_{i=1}^{6}\sum_{j=1}^{6} M_{ij}n_j e^i_{||}$$

$$=\tau g_{||}\ ,$$

$$g'_{\perp}=(-\tau^{-1})g_{\perp}\ .$$

Similarly, for a peak with odd-parity indices we find that application of M^3 inflates $g_{||}$ by τ^3 while deflating $g_{\perp}$ by $-\tau^{-3}$.

All this discussion can be summarized very simply. The set of all Bragg peaks can be grouped into two types according to parity. Every even-parity peak belongs to a sequence of the form

$$\tau^k g_{||},\quad k=0,\pm1,\pm2,\ldots$$

with the corresponding sequence of pseudospace vectors given by

$$(-\tau^{-1})^k g_{\perp},\quad k=0,\pm1,\pm2,\ldots .$$

Odd-parity peaks also fall into such sequences, except that τ should be replaced by τ^3. We notice (in both cases) that as the magnitude of the physical Bragg vector increases, the corresponding pseudospace vector diminishes in magnitude. The progression of $g_{\perp}$-dependent intensity values for such sequences is sketched in Fig. 7. We see that the peaks converging on the origin in $g_{||}$ space have rapidly decaying intensities. Moving in the opposite direction, outward from the origin, the intensities approach a con-

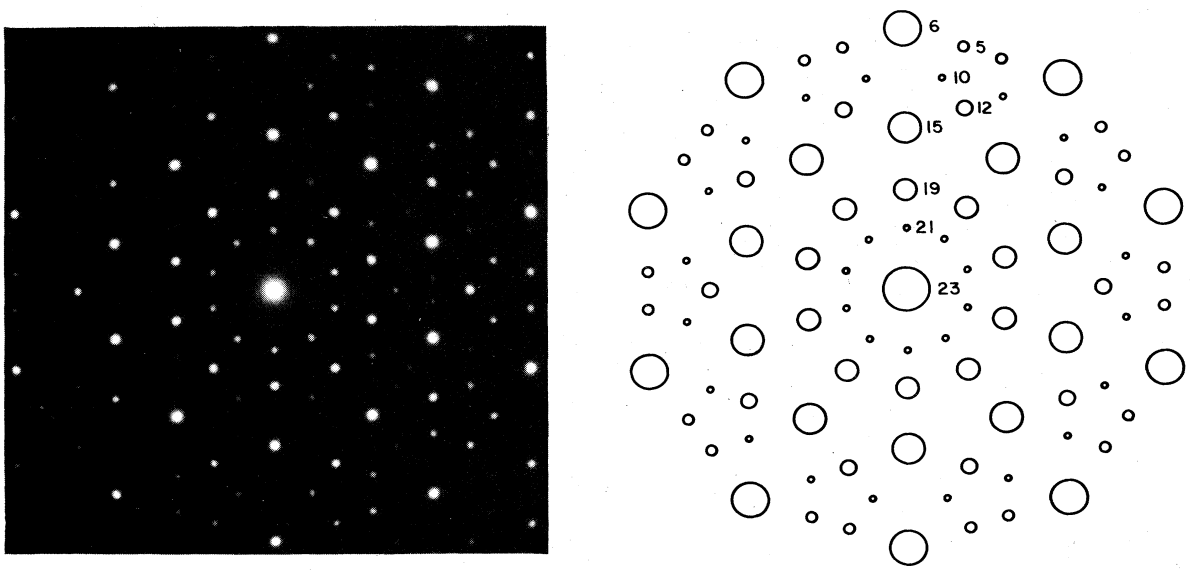

FIG. 11. Same as Fig. 9, but for the fivefold pattern.

stant value. Examples of these sequences in the electron-diffraction patterns of $Al_{0.86}Mn_{0.14}$ (Ref. 14) are shown in Fig. 8.

The above discussion applies most clearly to the primitive quasicrystal when complicating form factor effects are ignored. In this case the intensities are functions of $g_\perp$ only and contain all the relevant scale information. For the following it will be useful to express the intensity

$$I(g)=i(g_\perp a)=i(n_\perp)$$

in terms of the dimensionless pseudospace vector

$$n_\perp=\pi\sum_{i=1}^{6} n_i e_\perp^i \ .$$

From the formula[5]

$$i(n_\perp)\propto\left|\int\rho(x_\perp)e^{-in_\perp\cdot x_\perp}d^3x_\perp\right|^2, \tag{6}$$

$$\rho(x_\perp)=\begin{cases}1, & \text{if } x_\perp\in T\\ 0, & \text{otherwise}\end{cases} \tag{7}$$

where T is the triacontahedron of unit edge length, it is clear that $i(n_\perp)$ is appreciable only for $|n_\perp|\lesssim 1$ and decays rapidly beyond $|n_\perp|\approx 1$.

Now suppose g_{expt} is an experimental peak having the same angular position relative to the icosahedral axes as the quasicrystal peak with indices $(n_1,\ldots,n_6)$. To this peak we assign the intensity $i(n_\perp)$ and the quasilattice constant is found by solving the equation

$$g_{\text{expt}}=\frac{\pi}{a}\sum_{i=1}^{6} n_i e_{||}^i=\frac{n_{||}}{a}$$

for a. If the index has even parity, we know from the above that there is a whole sequence of alternative identifications given by

$$a'=\tau^k a,\quad n'_{||}=\tau^k n_{||},\quad n'_\perp=(-\tau^{-1})^k n_\perp \ , \qquad k=\pm1,\pm2,\ldots \tag{8}$$

with respective intensities $i(n'_\perp)$. To decide among these, one has to compare with the corresponding experimental intensities. This amounts to "shifting" one intensity sequence relative to another by rescaling with factors of τ.

Even when the intensity sequences do not give a perfect match due to form factor or $g_{||}$-dependent effects, it is probably still possible to identify a peak in the experimental sequence that marks the crossover to decaying behavior. For this peak one picks the term in the sequence (8) having $|n_\perp|\approx 1$ and then solves for a. A scale determination based on this approach might very likely be ambiguous up to a factor of τ. This suggests it is advantageous to choose instead an *odd*-parity sequence. Because successive terms in such sequences are related by factors of $\tau^3=4.236$, it is considerably easier to decide on the term having $|n_\perp|\approx 1$. Applying this strategy to the $Al_{0.86}Mn_{0.14}$ alloy we are led to identify an odd-parity peak of the twofold pattern (indicated by the arrow in Fig. 8) with the peak

$$|g_{||}|a=|n_{||}|=13.308 \ ,$$

$$|g_\perp|a=|n_\perp|=0.742$$

listed in Table I. Using the value $|g_{\text{expt}}|=|g_{||}|=2.896$ Å^{-1},[15] one finds $a=4.60$ Å. Figures 9–11 compare the twofold, threefold, and fivefold electron-diffraction patterns of $Al_{0.86}Mn_{0.14}$ with the primitive quasicrystal pattern adjusted to this value of the quasilattice constant.

In the above discussion it was assumed that the quasicrystal is not roughened in the sense described in Sec. II. This suggests a modification of the analysis to allow for the possibility that the pseudospace density $\rho(x_\perp)$ appearing in (6) is no longer of the ideal form given by (7). Roughening of the quasicrystal will lead to a broadened $\rho(x_\perp)$, possibly Gaussian with some width $\Delta x_\perp$. This implies that the intensity function $i(n_\perp)$ will now be concentrated over a smaller range than before, i.e., $\Delta n_\perp\lesssim(\Delta x_\perp)^{-1}$. As a result, the intensities in the sequences (8) will begin to decay at the point where $|n_\perp|$ is of order $(\Delta x_\perp)^{-1}$ rather than 1. It is not presently known how seriously one should consider this roughening possibility in the analysis of the $Al_{0.86}Mn_{0.14}$ diffraction data.

Note added. At the time of writing this paper the author received a copy of unpublished work by Bancel *et al.*[16] which gives an indexing scheme for icosahedral Al-Mn related to the present one by three deflations, i.e., a scale factor of τ^3.

ACKNOWLEDGMENT

The author thanks Chris Henley for having a sincere interest in the value of the quasilattice constant.

[1]D. Shechtman, I. Blech, D. Gratias, and J. W. Cahn, Phys. Rev. Lett. **53**, 1951 (1984).

[2]P. Kramer and R. Neri, Acta Crystallogr. Sect. A **40**, 580 (1984).

[3]D. Levine and P. J. Steinhardt, Phys. Rev. Lett. **53**, 2477 (1984).

[4]P. A. Kalugin, A. Yu. Kitaev, and L. C. Levitov, Pis'ma Zh. Eksp. Teor. Fiz. **41**, 119 (1985) [JETP Lett. **41**, 119 (1985)].

[5]V. Elser, Acta Crystallogr. Sect. A (to be published).

[6]M. Duneau and A. Katz, Phys. Rev. Lett. **54**, 2688 (1985).

[7]R. K. P. Zia and W. J. Dallas, J. Phys. A **18**, L341 (1985).

[8]The technique was first used for modulated crystal structures; see P. M. de Wolff, Acta Crystallogr. Sect. A **30**, 777 (1974).

[9]V. Elser, Phys. Rev. Lett. **54**, 1730 (1985).

[10]A phenomenological discussion of this point is given by D. R. Nelson and S. Sachdev, Phys. Rev. B **32**, 689 (1985).

[11]This deviates from the normalization of Ref. 5 by the factor $\sqrt{2}$.

[12]These terms were originally introduced by J. H. Conway to describe analogous transformations of the two-dimensional Penrose tiling. See M. Gardner, Sci. Am. **236**(1), 110 (1977).

[13]We note that $M=\tau P_{||}-\tau^{-1}P_\perp$ contains the two projection operators used in Ref. 5.

[14]The electron-diffraction patterns were taken by C. H. Chen from samples prepared by H. S. Chen.

[15]P. Horn (private communication).

[16]P. A. Bancel, P. A. Heiney, P. W. Stephens, A. I. Goldman, and P. M. Horn, Phys. Rev. Lett. **54**, 2422 (1985).

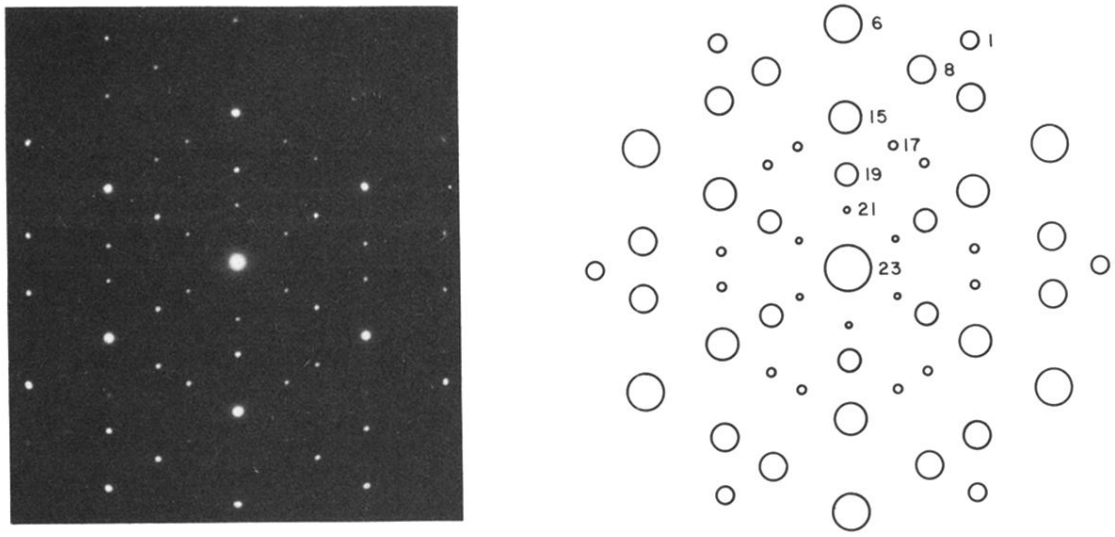

FIG. 10. Same as Fig. 9, but for the threefold pattern.

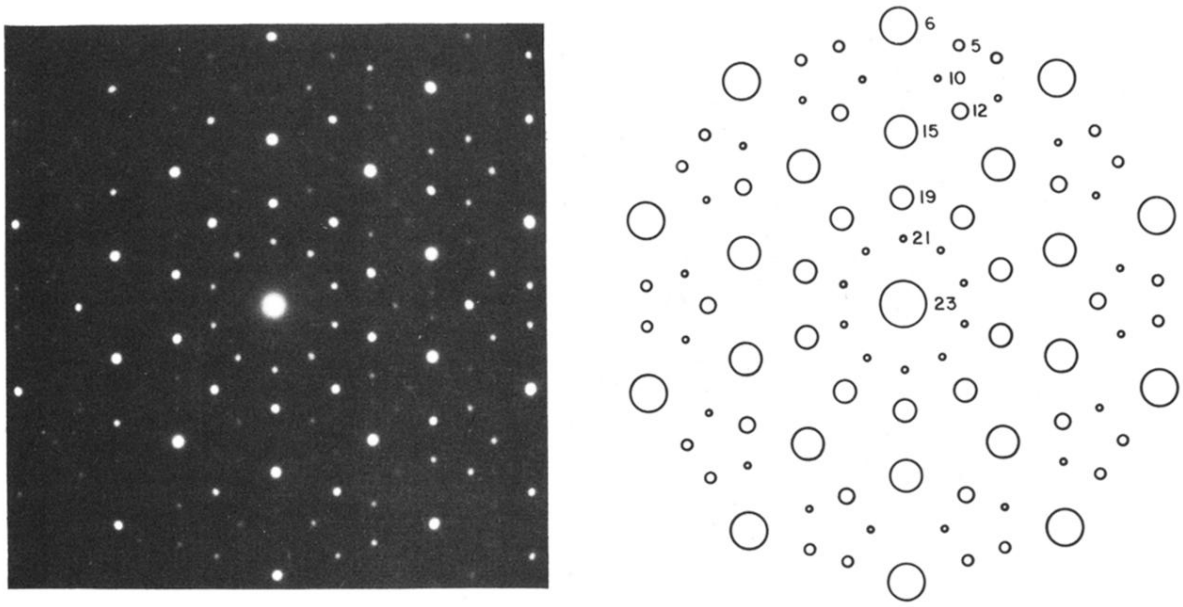

FIG. 11. Same as Fig. 9, but for the fivefold pattern.

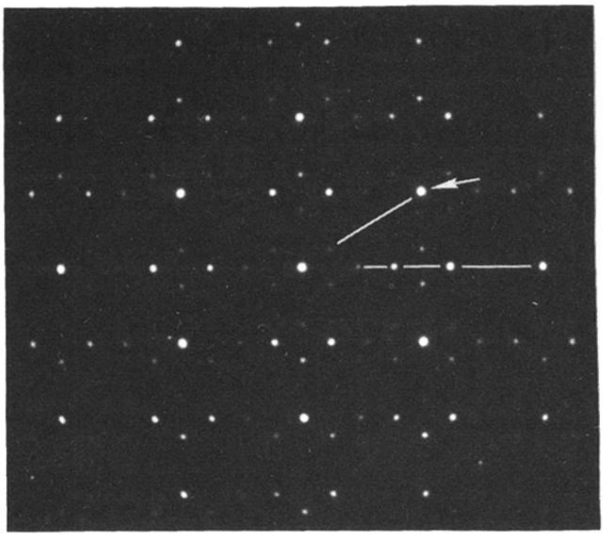

FIG. 8. Even- and odd-parity sequences in the experimental two-fold pattern (Ref. 14). The arrow indicates the peak at 2.896 Å^{-1}.

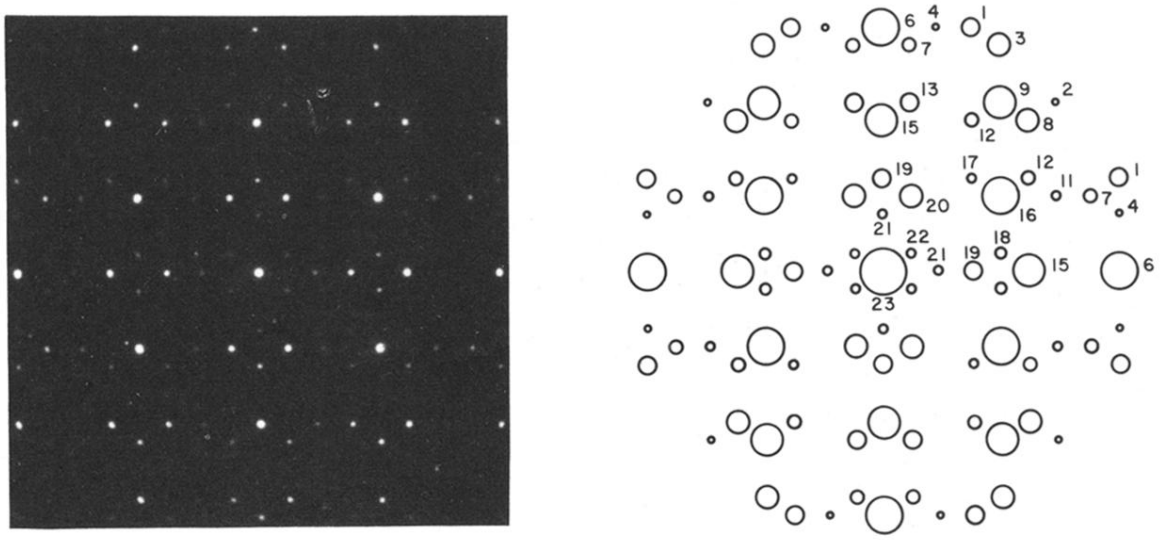

FIG. 9. Comparison of experimental (Ref. 14) and theoretical twofold patterns. The theoretical pattern is that of the primitive icosahedral quasicrystal with a rhombohedral edge length of 4.60 Å. Intensities are represented by the areas of the circles and the numerals refer to the listing of peaks in Table I.